This article has been accepted for publication in a future issue of this journal, but has not been fully edited. Content may change prior to final publication. Citation information: DOI 10.1109/TVT.2018.2837691, IEEE Transactions on Vehicular Technology

Differential Subcarrier Index Modulation

Saud Althunibat, *Member, IEEE*, Raed Mesleh, *Senior Member, IEEE* and Ertugrul Basar, *Senior Member, IEEE*

***Abstract*—One of the main challenges in orthogonal frequency division multiplexing (OFDM)–subcarrier index modulation (SIM) systems is the huge amount of resources required to obtain channel state information at the receiver side. In this paper, a differential subcarrier index modulation (DSIM) scheme is proposed, which entirely avoids the need for any channel knowledge at the receiver side. As such, time and energy resources spent in the channel estimation process are perceived. In DSIM, part of the transmitted block is modulated through ordinary signal modulation, whereas the second part is transmitted by selecting a specific permutation of the active subcarriers. The transmitted signals are designed to facilitate differential demodulation at the receiver side. A derivation is conducted for the average bit error probability of DSIM and an upper bound expression is obtained. Derived theoretical expression is substantiated through Monte Carlo simulation results. Reported results reveal that differential demodulation degrades the error performance of coherent SIM by nearly 4 dB in signal-to-noise-ratio.**

***Index Terms*—Coherent and non-coherent modulation, Index modulation, OFDM, Subcarrier index modulation, Differential modulation.**

I. Introduction

Index modulation (IM) is one of the promising transmission schemes for next-generation wireless communication systems due to its appealing advantages [1–4]. In IM, additional constellation diagrams are utilized to convey information bits and enhance the overall spectral efficiency. The indexes can be either spatially distributed transmit antennas as in space modulation techniques [5–9], orthogonal frequency division multiplexing (OFDM) subcarriers as in subcarrier index modulation (SIM) [10], signal polarizations as in polarization shift keying [11], or distributed relays as in dual-hop cooperative networks [2]. Generally in IM systems, the available indexes are treated as an extra constellation diagram and part of the incoming data bits modulate one or more of these indexes to be active at a particular time instant. It has been shown in the literature that IM systems provide several advantages as compared to traditional systems for the same spectral efficiency [2, 12].

In this study, we focus on SIM, also known as OFDM with IM (OFDM-IM), where a frame of OFDM subcarriers is divided into groups, each is in charge of transmitting a block of data bits. Part of the bits block is modulated through ordinary signal modulation, such as M-ary phase shift keying or quadrature amplitude modulation (M-PSK/QAM), while the other part modulates the indexes of the subcarriers within the group that will transmit the modulated symbols. Only a subgroup of the subcarriers within each group will be active and all other subcarriers will be switched off, i.e., transmitting no data. The receiver's task is to decode the active subcarriers within each group and the transmitted symbols on these subcarriers to retrieve the transmitted information bits.

Compared to classical OFDM, SIM benefits from the frequency selectivity to provide a better error performance at a given spectral efficiency [13]. As such, it has attracted significant research interest recently. A generalized SIM scheme is presented in [13], where the number of active subcarriers and the number of modulation bits are both changeable. In [14], the ergodic rate of SIM is investigated and maximized by optimizing the subcarrier activation strategy. In [15], it is shown that SIM is able to reduce the peak-to-average power ratio (PAPR) compared to OFDM, while in [16], the inactive subcarriers are exploited to further reduce the PAPR using convex programming. A tight approximation on the average bit error rate (BER) of SIM is derived in [17]. The complexity reduction at the detectors of SIM is investigated in [18–20]. The optimal number of subcarrier groups and active subcarriers are optimized for maximum spectral and energy efficiencies in [21] and [22], respectively. Recently, several enhanced SIM variants also appeared in the literature to obtain improved spectral efficiency as well as error performance [23–26].

In all previous SIM schemes, channel state information (CSI) is required at the receiver for optimum detection. Such CSI knowledge is attained through periodic channel estimation process for each transmitted frame. The channel estimation exhausts the limited resources and the errors in channel estimation deteriorate the overall system performance. Designing a non-coherent scheme for SIM is very sophisticated considering the working mechanism of SIM, in which data is conveyed through activating certain subcarriers within a group to transmit modulated symbols.

In this paper, we propose differential SIM (DSIM) by utilizing the ideas in the recently proposed non-coherent schemes for space modulation systems, such as differential spatial modulation (DSM) [27–31], differential quadrature spatial modulation (DQSM) [32], and differential space-frequency block code-OFDM (DSFBC-OFDM) [33], which applies differential space-time coding techniques to OFDM subcarriers [34]. To the best of the authors' knowledge, differential schemes for SIM do not yet exist in the literature. The proposed DSIM scheme relies on a permutation of N subcarriers over N consecutive time slots to convey information bits. An upper bound of the average bit error rate (BER) is derived for the proposed DSIM scheme. Analytical results are validated

Saud Althunibat is with Al-Hussein Bin Talal University, Maan, Jordan, (e-Mail: saud.althunibat@ahu.edu.jo.)

Raed Mesleh is with the Electrical and Communication Engineering Department, School of Electrical Engineering and Information Technology, German Jordanian University, Amman 11180, Jordan (e-mail: raed.mesleh@gju.edu.jo.)

E. Basar is with Istanbul Technical University, Faculty of Electrical and Electronics Engineering, 34469, Istanbul, Turkey (e-mail: basarer@itu.edu.tr).

This article has been accepted for publication in a future issue of this journal, but has not been fully edited. Content may change prior to final publication. Citation information: DOI 10.1109/TVT.2018.2837691, IEEE Transactions on Vehicular Technology

through Monte Carlo simulation results, which demonstrate close-match for wide and pragmatic range of signal-to-noise-ratio (SNR) values. In addition, the performance of DSIM is compared to coherent SIM assuming perfect CSI knowledge at the receiver side for the same spectral efficiency and performance degradation of about 3-4 dB is reported.

The rest of the paper is organized as follows. Section II reviews the coherent SIM scheme. The proposed DSIM scheme is presented in Section III. Performance analysis is conducted in Section IV. In Section V, computer simulation and analytical results are provided and thoroughly discussed. Conclusions are drawn in Section VI.

II. Subcarrier Index Modulation (SIM) Overview

An OFDM system with SIM is considered as shown in Fig. 1, where the total system bandwidth consists of L subcarriers, which are grouped in G groups. Hence, the number of subcarriers in each group, denoted by N, is $N = \frac{L}{G}$.

Without loss of generality, it is assumed that N is a power of two integer number (i.e., 2, 4, 8, ...), and only a single subcarrier is activated in each group. As a result, the transmitted block at each transmit symbol duration contains B bits in SIM, where B is expressed as

$$B = G\left(\log_2\left(M\right) + \log_2\left(N\right)\right), \tag{1}$$

with M being the modulation order of an arbitrary constellation diagram such as PSK/QAM or any other constellation diagram. The transmitted block is divided into G sub-blocks, where the g^{th} sub-block is to be transmitted by the g^{th} group (for $g = 1, 2, 3, ..., G$).

Let the bits to be modulated on the g^{th} sub-block are denoted as $\mathbf{b}_g = \{b_{g1}, b_{g2}, ..., b_{gk}\}$, where $k = \log_2(M) + \log_2(N)$ being the total number of bits in each sub-block. SIM implies that the first $\log_2 M$ bits modulate and ordinary complex symbol drawn from the considered $M-$PSK/QAM constellation diagram. The modulated symbol in each group is transmitted by a single subcarrier determined by the remaining $\log_2 N$ bits in the transmitted sub-block. The same procedure is repeated for each sub-block until the whole OFDM block, with B bits, is delivered. At the receiver, maximum likelihood (ML) decoder is considered assuming the full channel state information to retrieve the transmitted data[1].

III. Differential SIM (DSIM)

The availability of the CSI at the receiver in SIM system is a major requirement for ML detection. However, such necessity costs a continuous resource expenditure for both the transmitter and the receiver represented by the periodic channel estimation process and the accompanying overhead, which consumes energy, time and throughput. In what follows, a novel DSIM scheme is proposed, which alleviates the need for any channel knowledge at the receiver side and transmitted data can be estimated by differentially modulating the transmit signals.

[1]Readers may refer to [10] for a detailed performance analysis of OFDM-IM system.

The proposed DSIM scheme is illustrated in Fig. 2. In DSIM, the available subcarriers are divided to G groups with each group containing N subcarriers similar to SIM. The transmitted block from each group conveys D bits that are transmitted over N time slots, where D is given by

$$D = \lfloor \log_2\left(N!\right) \rfloor + N\log_2\left(M\right), \tag{2}$$

with $(\cdot)!$ denoting the factorial operator. From (2), a total of GD bits will be transmitted over N time slots from all subcarriers in the G groups.

The proposed DSIM scheme implies that the first $\lfloor \log_2\left(N!\right) \rfloor$ bits are used to determine the permutation of the active subcarriers of the corresponding group over N time slots. To facilitate differential modulation and demodulation, the allowed permutations for the active subcarriers must fulfill the following two conditions:

1) Only a single subcarrier within each group is activated at each particular time slot.
2) A subcarrier is activated only once over an N time slots.

A mapping table with all possible permutations for $N = 4$ while satisfying the previous two conditions is enclosed in Fig. 2.

It should be mentioned that there exist some schemes in the literature that relaxes the above conditions and design DSM with arbitrary QAM and APSK constellations [35, 36]. Designing the proposed DSIM with modulation orders rather than PSK should be theoretically possible but requires substantial design and analysis and is an interesting research topic for future investigations.

The remaining $N \log_2 M$ bis in the block modulate N symbols from an arbitrary $M-$PSK constellation diagram. At each time slot, the modulated symbols are transmitted by the active subcarriers determined by the selected permutation.

Considering the g^{th} subcarrier group, the modulated symbols of the w^{th} block ($w = 1, 2, ...$) over N time slots are formulated in the matrix $\mathbf{X}_w^g$ as

$$\mathbf{X}_w^g = \begin{bmatrix} x_{11} & x_{12} & \cdots & x_{1N} \\ x_{21} & x_{22} & \cdots & x_{2N} \\ \vdots & \vdots & \cdots & \vdots \\ x_{N1} & x_{N2} & \cdots & x_{NN} \end{bmatrix}, \tag{3}$$

where x_{nt} represents the modulated symbol on the n^{th} subcarrier at the t^{th} time slot (for t and $n \in \{1, \ldots, N\}$). Please note that each column of $\mathbf{X}_w^g$ has only one non-zero element to fulfill the conditions of DSIM. Recall that only one subcarrier from each group is activated, and it is activated only once during the block transmission (i.e., N time slots).

The facilitate differential modulation, the transmitted matrix from the g^{th} group over N time slots, denoted by $\mathbf{S}_w^g$, depends not only on the current signal, but also on the previous one as

$$\mathbf{S}_w^g = \mathbf{S}_{w-1}^g \mathbf{X}_w^g, \tag{4}$$

where $\mathbf{S}_{w-1}^g$ is the transmitted matrix of the previous block, which is initially assumed to be an identity matrix (*i.e.,* $\mathbf{S}_{-1}^g = \mathbf{I}_N$, where $\mathbf{I}_N$ denotes an $N-$dimensional identity matrix). Let $\mathcal{S}$ be a set of all possible transmitted matrices. For DSIM, the closure property must be fulfilled such that if $\mathbf{X}_w^g \in \mathcal{S}$

This article has been accepted for publication in a future issue of this journal, but has not been fully edited. Content may change prior to final publication. Citation information: DOI 10.1109/TVT.2018.2837691, IEEE Transactions on Vehicular Technology

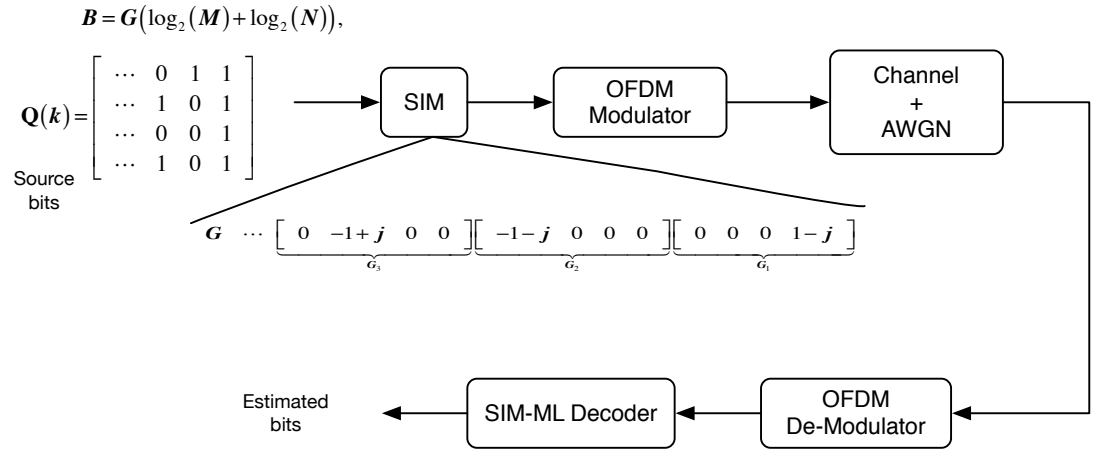

Fig. 1. SIM system model with an example of data bits mapping procedure assuming $N = 4$ and $M = 4-$QAM.

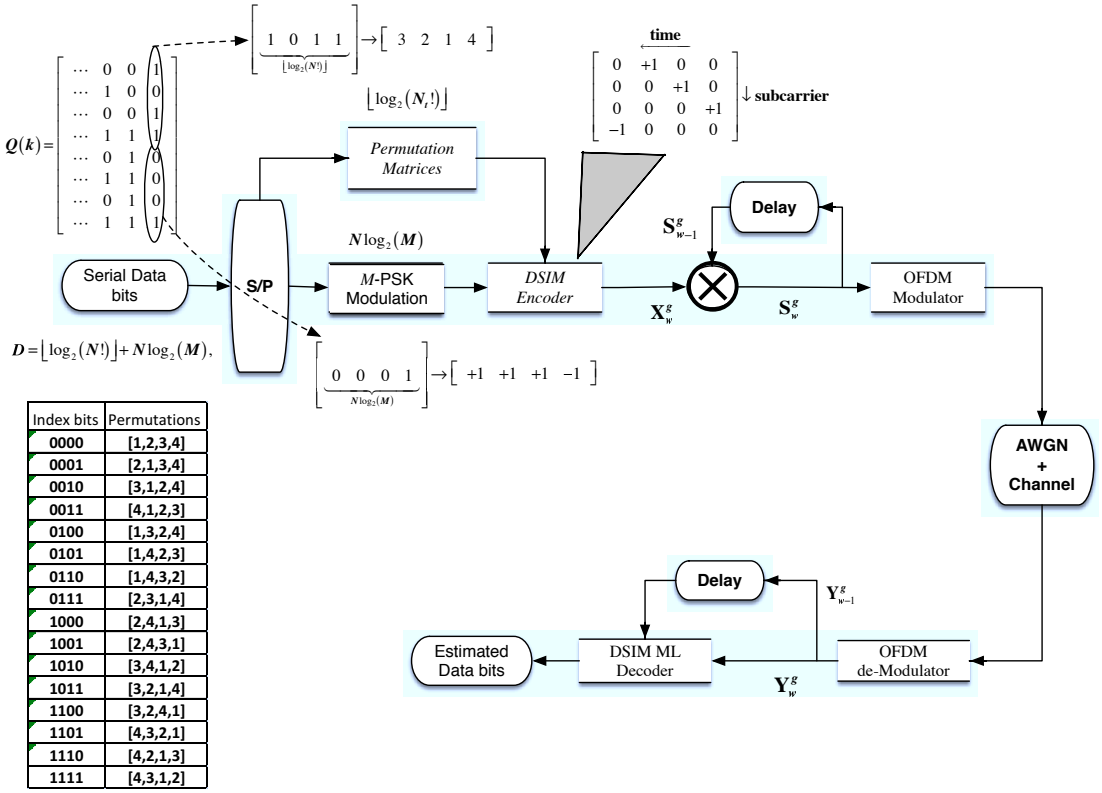

Index bits	Permutations
0000	[1,2,3,4]
0001	[2,1,3,4]
0010	[3,1,2,4]
0011	[4,1,2,3]
0100	[1,3,2,4]
0101	[1,4,2,3]
0110	[1,4,3,2]
0111	[2,3,1,4]
1000	[2,4,1,3]
1001	[2,4,3,1]
1010	[3,4,1,2]
1011	[3,2,1,4]
1100	[3,2,4,1]
1101	[4,3,2,1]
1110	[4,2,1,3]
1111	[4,3,1,2]

Fig. 2. The proposed DSIM system model with an illustrating example assuming $N = 4$ and BPSK modulation. A mapping table with possible permutation of N subcarriers is enclosed in the figure as well. S/P denotes the serial-to-parallel operation.

and $\mathbf{S}_{w-1}^g \in \mathcal{S}$, the multiplication of $\mathbf{S}_w^g = \mathbf{S}_{w-1}^g \mathbf{X}_w^g \in \mathcal{S}$. To achieve this, the non-zero elements of $\mathbf{X}_w^g$ and $\mathbf{S}_w^g$ must have unity amplitudes, i.e., obtained from a PSK constellation diagram.

The elements of the generated matrix, $\mathbf{S}_w^g$, are rearranged in a vector with NG dimension before being modulated by an OFDM modulator and transmitted over a frequency selective fading channel with ν taps whose channel impulse response is given by

$$\mathbf{h}_t = \begin{bmatrix} h_1 & h_2 & \cdots & h_\nu \end{bmatrix}^T, \tag{5}$$

where $(\cdot)^T$ denotes the transpose operation. The entries of $\mathbf{h}_t$ are assumed to be circularly symmetric complex Gaussian random variables with zero mean and $\frac{1}{\nu}$ variance.

At the receiver, the received signal is first demodulated through an OFDM demodulator and the matrix of the w^{th} block from the g^{th} group, denoted by $\mathbf{Y}_w^g$, is expressed as

$$\mathbf{Y}_w^g = \mathbf{H}_w^g \mathbf{S}_w^g + \mathbf{Z}_w^g, \tag{6}$$

where $\mathbf{Z}_w^g$ is an $N \times N$ additive white Gaussian noise (AWGN) matrix composed of i.i.d. elements with zero mean and σ_n^2 variance, and $\mathbf{H}_w^g$ is the $N \times N$ all zero matrix except its diagonal elements that equal the frequency-domain channel

This article has been accepted for publication in a future issue of this journal, but has not been fully edited. Content may change prior to final publication. Citation information: DOI 10.1109/TVT.2018.2837691, IEEE Transactions on Vehicular Technology

coefficients of the g^{th} subcarrier group.

The received signal matrix given in (6) can be rewritten by using (4) as

$$\mathbf{Y}_w^g = \mathbf{H}_w^g S_{w-1}^g \mathbf{X}_w^g + \mathbf{Z}_w^g, \tag{7}$$

and the received signals of the previous block can be expressed as

$$\mathbf{Y}_{w-1}^g = \mathbf{H}_{w-1}^g S_{w-1}^g + \mathbf{Z}_{w-1}^g. \tag{8}$$

In this study, a quasi static fading channel is considered, where the frequency channel response for each transmitted group of subcarriers is assumed to remain constant over two consecutive blocks (i.e., $\mathbf{H}_w^g = \mathbf{H}_{w-1}^g = \mathbf{H}^g$) [27, 32]. As such, the ML differential detection can be formulated as

$$\widehat{\mathbf{X}}_w^g = \arg \min_{\mathbf{X} \in \mathcal{X}} \left\| \mathbf{Y}_w^g - \mathbf{Y}_{w-1}^g \mathbf{X} \right\|_F^2, \tag{9}$$

where $\mathbf{X}$ refers to the possible matrix $\mathbf{X}_w^g$, $\mathcal{X}$ represents a set of all possible values of $\mathbf{X}$ and $\| \cdot \|_F^2$ denotes the Frobenius norm. With the aid of (7) and (8), (9) can be further simplified to

$$\hat{\mathbf{X}}_w = \arg \min_{\mathbf{X} \in \mathcal{X}} \left\| \mathbf{H}\mathbf{S}_{w-1} \left(\mathbf{X}_w - \mathbf{X} \right) + \mathbf{Z}_w - \mathbf{Z}_{w-1}\mathbf{X} \right\|_F^2, \tag{10}$$

where the g index is dropped in (10) to indicate that similar procedure is valid for all subcarrier groups. Upon obtaining $\hat{\mathbf{X}}_w$, it is re-mapped to the corresponding bits block.

A. An illustrative example

Let the total number of subcarriers be $L = 128$, which is divided into $G = 32$ groups, where each group contains $N = 4$ subcarriers and each active subcarrier carrying a BPSK symbol. The transmitted bits are divided into blocks each containing $D = 8$ bits and transmitted by a single group over $N = 4$ time slots.

Assume that a specific bits block is 10110001 as shown in Fig. 2. The first $\lfloor \log_2 (N!) \rfloor = 4$ bits (1011) will select the permutations of active subcarriers over 4 time slots. Considering the mapping table in Fig. 2 with $2^4 = 16$ different permutations that satisfy the conditions of DSIM, the permutation of the bits 1011 is $[3, 2, 1, 4]$, which indicates that only the third, second, first and fourth subcarriers are active during the consecutive four time slots. The remaining 4 bits in the block (0001) are modulated using BPSK modulation to the following symbols $[+1, +1, +1, -1]$. As such, $\mathbf{X}_w$ is formulated as

$$\mathbf{X}_w = \begin{bmatrix} 0 & +1 & 0 & 0 \\ 0 & 0 & +1 & 0 \\ 0 & 0 & 0 & +1 \\ -1 & 0 & 0 & 0 \end{bmatrix}. \tag{11}$$

The transmitted signal matrix, $\mathbf{S}_w$, is then obtained by multiplying $\mathbf{X}_w$ with $\mathbf{S}_{w-1}$. The process is repeated until modulating all $L = 128$ subcarriers, which are modulated through an OFDM modulator and transmitted over the channel. The receiver will apply the ML DSIM decoder to estimate the considered permutation for each group and the transmitted symbols on each active subcarrier. Estimated data are used to retrieve original information bits considering an inverse mapping procedure to that considered at the transmitter.

IV. Spectral Efficiency and Performance Analysis

A. Spectral Efficiency Analysis

The spectral efficiency in bits/s/Hz for SIM systems is given by [10]

$$\eta_{\text{SIM}} = \frac{B}{L + C}, \tag{12}$$

where C is the length of the cyclic prefix added at the transmitter. Consequently, the spectral efficiency of the proposed DSIM is expressed as

$$\eta_{\text{DSIM}} = \frac{GD}{N(L + C)}, \tag{13}$$

where D is the number of bits per group for DSIM as given in (2).

Aiming at quantifying the spectral efficiency loss, we define $\Delta = \eta_{\text{SIM}} - \eta_{\text{DSIM}}$, which is given by

$$\Delta = \frac{NB - GD}{N(L + C)}. \tag{14}$$

By substituting the values of B and D given respectively in (1) and (2) and canceling the identical terms, (14) can be rewritten as

$$\Delta = \frac{G \left(N \log_2 (N) - \lfloor \log_2 (N!) \rfloor \right)}{N \left(L + C \right)}, \tag{15}$$

which can be simplified by ignoring the floor operator to

$$\Delta \approx \frac{G \log_2 \left(\frac{N^N}{N!} \right)}{N \left(L + C \right)}. \tag{16}$$

The value of $N!$ can be further simplified using Stirling's formula [37] to $N! \approx \sqrt{2\pi N} N^N e^{-N}$, which when substituted in (16) leads to

$$\begin{aligned} \Delta \approx & \frac{G \log_2 \left(\frac{1}{\sqrt{2\pi N} e^{-N}} \right)}{N \left(L + C \right)} \\ = & \frac{-G \log_2 \left(\sqrt{2\pi N} e^{-N} \right)}{N \left(L + C \right)} \\ = & \frac{NG \log_2 (e) - G \log_2 \left(\sqrt{2\pi N} \right)}{N \left(L + C \right)} \\ = & \frac{L \log_2 (e)}{N \left(L + C \right)} - \frac{L \log_2 \left(\sqrt{2\pi N} \right)}{N^2 \left(L + C \right)}. \end{aligned} \tag{17}$$

Hence, the spectral efficiency loss is upper bounded by $\frac{L \log_2 (e)}{N(L+C)}$.

B. Performance analysis of the average BER

The BER performance of the proposed DSIM scheme is evaluated hereinafter. The error probability for all groups is identical. Hence, we focus on deriving the average error probability of a single group. The average BER can be computed

This article has been accepted for publication in a future issue of this journal, but has not been fully edited. Content may change prior to final publication. Citation information: DOI 10.1109/TVT.2018.2837691, IEEE Transactions on Vehicular Technology

through the well-known union-bound technique as [39]

$$\text{BER} \leq \frac{1}{2^D} \sum_{i=1}^{2^D} \sum_{j=1, j\neq i}^{2^D} \frac{e_{i,j}}{D} \text{PEP}_{i,j}, \tag{18}$$

where $\text{PEP}_{i,j}$ is the average pair-wise probability (PEP) of $\mathbf{X}_j$ being detected given that $\mathbf{X}_i$ is transmitted and $e_{i,j}$ is the hamming distance corresponding to this pairwise error event.

From (9), $\text{PEP}_{i,j}$ can be expressed as

$$\text{PEP}_{i,j} = \Pr\left\{ \|\mathbf{Y}_w^g - \mathbf{Y}_{w-1}\mathbf{X}_i\|_F^2 > \|\mathbf{Y}_w - \mathbf{Y}_{w-1}\mathbf{X}_j\|_F^2 \right\}. \tag{19}$$

Using (10), the left hand side of (19) can be reduced to

$$\text{PEP}_{i,j} = \Pr\left\{ \|\mathbf{Z}_w - \mathbf{Z}_{w-1}\mathbf{X}_i\|_F^2 > \|\mathbf{D}\Delta + \mathbf{Z}_w - \mathbf{Z}_{w-1}\mathbf{X}_j\|_F^2 \right\}, \tag{20}$$

where $\mathbf{D} = \mathbf{H}\mathbf{S}_w$ and $\mathbf{\Delta} = \mathbf{X}_i - \mathbf{X}_j$.

Expanding the norms reduces (20) to

$$\begin{aligned}\text{PEP}_{i,j} = \\ \Pr\Big\{ &\|\mathbf{Z}_w\|^2 + \|\mathbf{Z}_{w-1}\mathbf{X}_i\|^2 - 2\Re\left\{\text{Tr}\left(\mathbf{Z}_w^H\mathbf{Z}_{w-1}\mathbf{X}_i\right)\right\} > \\ &\|\mathbf{D}\Delta\|^2 + 2\Re\left\{\text{Tr}\left((\mathbf{D}\Delta)^H(\mathbf{Z}_w - \mathbf{Z}_{w-1}\mathbf{X}_j)\right)\right\} + \|\mathbf{Z}_w\|^2 \\ &-2\Re\left\{\text{Tr}\left(\mathbf{Z}_w^H\mathbf{Z}_{w-1}\mathbf{X}_j\right)\right\} + \|\mathbf{Z}_{w-1}\mathbf{X}_j\|^2\Big\}\end{aligned} \tag{21}$$

where $\Re\{\cdot\}$ denotes the real part of a complex number, $\text{Tr}(\cdot)$ is the matrix trace operator, and $(\cdot)^H$ denotes the Hermitian operation. Notice that $\|\mathbf{Z}_{w-1}\mathbf{X}_i\|^2 = \|\mathbf{Z}_{w-1}\mathbf{X}_j\|^2$ so they are canceled to simplify (21) to

$$\begin{aligned}\text{PEP}_{i,j} = \Pr\Big\{ &-2\Re\left\{\text{Tr}\left(\mathbf{Z}_w^H\mathbf{Z}_{w-1}\Delta + \right.\right. \\ &\left.\left.(\mathbf{D}\Delta)^H(\mathbf{Z}_w - \mathbf{Z}_{w-1}\mathbf{X}_j)\right)\right\} > \|\mathbf{D}\Delta\|_F^2\Big\}.\end{aligned} \tag{22}$$

The term $\mathbf{Z}_w^H\mathbf{Z}_{w-1}$ is a product of two complex Gaussian random matrices and the variance of the elements of the resultant matrix approaches zero at high SNR values [39]. Accordingly, neglecting the term $\mathbf{Z}_w^H\mathbf{Z}_{w-1}\mathbf{\Delta}$ approximates (22) to

$$\begin{aligned}\text{PEP}_{i,j} \approx \Pr\Big\{ &\Big\{-2\Re\left\{\text{Tr}\left((\mathbf{D}\Delta)^H(\mathbf{Z}_w - \mathbf{Z}_{w-1}\mathbf{X}_j)\right)\right\} \\ &> \|\mathbf{D}\Delta\|^2\Big\}\Big\}.\end{aligned} \tag{23}$$

For a given $\mathbf{H}$, the left-hand side is actually a Gaussian random variable with zero mean and a variance of $4\|\mathbf{D}\mathbf{\Delta}\|^2\sigma_n^2$. Therefore, the conditional $\text{PEP}_{i,j}$ on $\mathbf{H}$ can be expressed using the Q-function as

$$\begin{aligned}\text{PEP}_{i,j/\mathbf{H}} &\approx Q\left(\frac{\|\mathbf{D}\Delta\|^2}{\sqrt{4N\|\mathbf{D}\Delta\|^2\sigma_n^2}}\right) \\ &\approx Q\left(\sqrt{\frac{\|\mathbf{D}\Delta\|^2}{4N\sigma_n^2}}\right) \\ &\approx \frac{1}{2\pi}\int_0^{\frac{\pi}{2}} \exp\left(\frac{\|\mathbf{D}\Delta\|^2}{4N\sigma_n^2\sin\theta}\right) d\theta,\end{aligned} \tag{24}$$

where the last expression is obtained by using the Craig's formula of the Q-function [40].

Now, the unconditional PEP_{ij} can be obtained by taking the expectation of both sides as

$$\text{PEP}_{i,j} \approx \frac{1}{2\pi}\int_0^{\frac{\pi}{2}} \text{E}\left[\exp\left(-\frac{\|\mathbf{D}\Delta\|^2}{4N\sigma_n^2\sin\theta}\right) d\theta\right]. \tag{25}$$

The integral in (25) represents the moment generation function (MGF) of the random variable $\|\mathbf{D}\mathbf{\Delta}\|^2$ for the value of $\frac{-1}{4N\sigma_n^2\sin\theta}$ (i.e, MGF $\left(\frac{-1}{4N\sigma_n^2\sin\theta}\right)$). Thus, it can be rewritten as

$$\text{PEP}_{i,j} \approx \frac{1}{2\pi}\int_0^{\frac{\pi}{2}} \text{MGF}\left(\frac{-1}{4N\sigma_n^2\sin\theta}\right) d\theta. \tag{26}$$

According to [41], the MGF for the variable α is given by

$$\text{MGF}(\alpha) = \frac{\exp\left(\alpha\overline{\mathbf{D}}^H\Psi(\mathbf{I}_{N^2} - \alpha\mathbf{C}_\mathbf{D}\Psi)^{-1}\overline{\mathbf{D}}\right)}{\det\left(\mathbf{I}_{N^2} - \alpha\mathbf{C}_\mathbf{D}\Psi\right)}, \tag{27}$$

where $\overline{\mathbf{D}}$ and $\mathbf{C}_\mathbf{D}$ are respectively the mean vector and the covariance matrix of $\text{vec}\left(\mathbf{D}^H\right)$ with $\text{vec}(\cdot)$ denoting the vectorization operator, $\mathbf{\Psi} = \mathbf{I}_N \otimes \mathbf{\Delta}\mathbf{\Delta}^H$, $\otimes$ is the Kronecker product, and $\det(\cdot)$ is the determinant operator.

By replacing $\alpha = \frac{-1}{4N\sigma_n^2\sin\theta}$, and substituting the result into (26), the integral can be upper bounded by letting $\theta = \pi/2$ as

$$\text{PEP}_{i,j} \leqslant \frac{1}{2}\frac{\exp\left(\delta\overline{\mathbf{D}}^H\Psi(\mathbf{I}_{N^2} + \delta\mathbf{C}_\mathbf{D}\Psi)^{-1}\overline{\mathbf{D}}\right)}{\det\left(\mathbf{I}_{N^2} + \delta\mathbf{C}_\mathbf{D}\Psi\right)}, \tag{28}$$

where $\delta = \frac{1}{4N\sigma_n^2}$. For Rayleigh fading, $\overline{\mathbf{D}}$ is expressed as follows

$$\begin{aligned}\overline{\mathbf{D}} &= \text{E}\left[\text{vec}\left(\mathbf{D}^H\right)\right] \\ &= \text{E}\left[\text{vec}\left(\mathbf{H}^H\mathbf{S}_w^H\right)\right] \\ &= \text{E}\left[\text{vec}\left(\mathbf{H}^H\right)\right]\text{E}\left[\text{vec}\left(\mathbf{S}_w^H\right)\right] \\ &= \mathbf{0}_{N^2}\end{aligned} \tag{29}$$

where $\mathbf{0}_{N^2}$ is an $N^2 \times N^2$ all-zero square matrix. The last equality in (29) refers to the fact that Rayleigh fading has zero mean in time and frequency domains. Using (29), the upper bound derived in (28) can be further reduced to

$$\text{PEP}_{i,j} \leqslant \frac{1}{2}\frac{1}{\det\left(\mathbf{I}_{n^2} + \delta\mathbf{C}_\mathbf{D}\Psi\right)}. \tag{30}$$

To compute the covariance matrix $\mathbf{C}_\mathbf{D}$, we consider the correlation matrix of $\mathbf{h}^F$, which is given by

$$\begin{aligned}\mathbf{G} &= \text{E}\left\{\mathbf{h}^F(\mathbf{h}^F)^H\right\} \\ &= \text{E}\left\{\mathbf{F}\mathbf{h}^T\mathbf{h}^F\mathbf{F}^H\right\} \\ &= \mathbf{F}\text{E}\left\{\mathbf{h}^T(\mathbf{h}^F)^H\right\}\mathbf{F}^H \\ &= \mathbf{F}\mathbf{J}\mathbf{F}^H,\end{aligned} \tag{31}$$

where $\mathbf{J}$ is an $L \times L$ all-zero matrix except the first ν elements in its diagonal, which equal $\frac{1}{\nu}$. Accordingly, $\mathbf{C}_\mathbf{D}$ is defined as an $N^2 \times N^2$ matrix centered along the main diagonal of $\mathbf{G}$.

This article has been accepted for publication in a future issue of this journal, but has not been fully edited. Content may change prior to final publication. Citation information: DOI 10.1109/TVT.2018.2837691, IEEE Transactions on Vehicular Technology

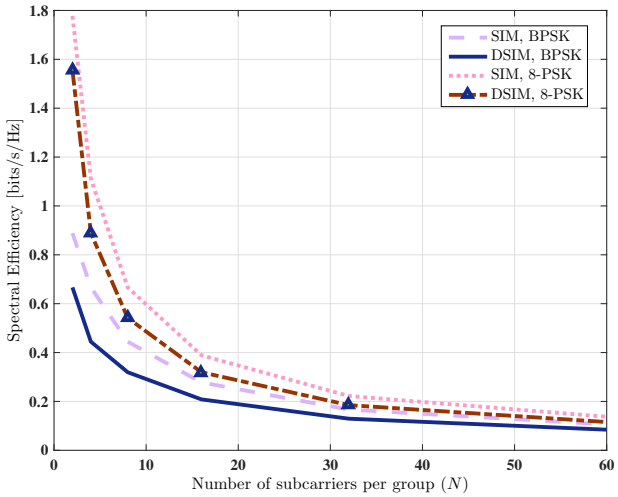

Fig. 3. The achievable spectral efficiency versus the number of subcarriers per group for SIM and DSIM for different modulation orders. ($L = 128$, $\nu = 10$, $C = 16$.).

V. Simulation Results

An OFDM system with $L = 128$ subcarriers is assumed to be operating over a frequency selective fading channel with $\nu = 10$ taps and the length of the cyclic prefix is set to $C = 16$. The average SNR is defined as the ratio of the energy-per-bit $\left(E_b = \frac{L+C}{GD/N}\right)$ to the noise power in time domain $\left(\frac{G}{N}\sigma_n^2\right)$ [10].

The spectral efficiency versus the number of subcarriers per group, N, for both SIM and DSIM at two different modulation orders is depicted in Fig. 3. Only a single subcarrier per group is activated in SIM. As anticipated, the overall spectral efficiency for both systems decreases as N increases. This can be explained by the fact that increasing N, decreases the number of groups, G, which consequently decreases the length of the transmitted block. In addition, it is noted that the spectral efficiency loss between SIM and DSIM systems diminishes as N increases, which can be clearly noted from (17). Also, the spectral efficiency loss is independent of the modulation order M, where using BPSK and 8PSK result in the same spectral efficiency loss at a specific value of N. For example, assuming BPSK or 8PSK, the spectral efficiency loss is 0.2222 bps/Hz at $N = 2$ while it decreases to 0.0373 bps/Hz at $N = 32$.

The average BER versus the average SNR is plotted in Fig. 4 for SIM and DSIM at a spectral efficiency of 0.6667 bits/s/Hz. The given spectral efficiency is achieved with $N = 4$ and a single active subcarrier for SIM and with $N = 2$ for DSIM while using BPSK modulation, ($M = 2$). It can be clearly seen from Fig. 4 that differential modulation results in about 4 dB loss as compared to coherent detection, which is acceptable considering the simplicity of the DSIM receiver.

At a spectral efficiency of 0.4444 bits/s/Hz, Fig. 5 plots the average BER versus the average SNR for both systems. The target spectral efficiency is accomplished with $N = 8$, $M = 2$ and $N = 4$, $M = 2$ for SIM and DSIM, respectively. Again, only a single subcarrier per group is activated in SIM.

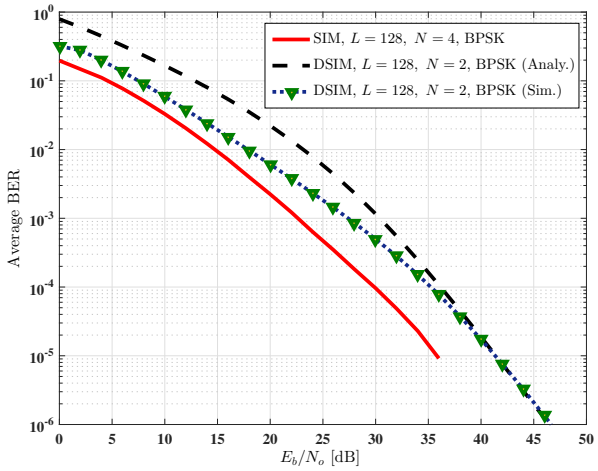

Fig. 4. The average BER versus E_b/N_0 for SIM and DSIM at a spectral efficiency of 0.6667 bps/Hz. ($L = 128$, $\nu = 10$, $C = 16$).

Similar to Fig. 4, a 4 dB degradation in SNR is reported when comparing DSIM and SIM results. From Figs. 4-5, we also observe that the provided analytical upper bounds become considerable tight for higher SNR values.

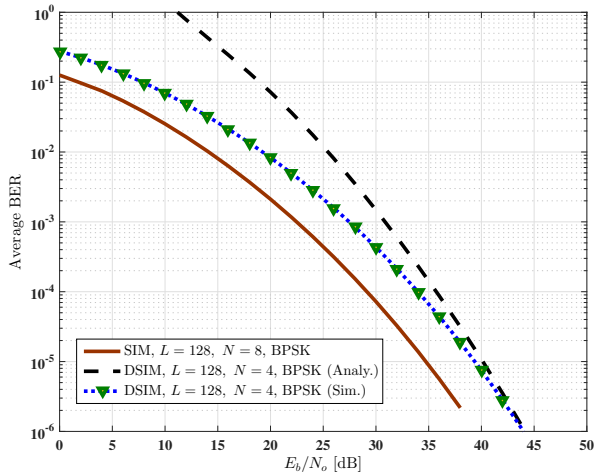

Fig. 5. The average BER versus E_b/N_o for IM-OFDM and DIM-OFDM at a spectral efficiency of 0.4444 bps/Hz. ($L = 128$, $\nu = 10$, $C = 16$).

The results at a spectral efficiency of 2 bits/s/Hz for both SIM and DSIM systems are shown in Fig. 6. For SIM, 2 bits/s/Hz can be achieved by $N = 4$ and $M = 128$, while for DSIM, the same spectral efficiency can be achieved by $N = 2$ and $M = 16$. Unlike Fig. 4 and Fig. 5, the SNR degradation is reduced to about 2 dB. This due to adopting a high modulation order ($M = 128$) in SIM, which causes a slight performance degradation in average BER for IM systems [26].

The performance of conventional differential-PSK over OFDM systems (DPSK-OFDM) compared to the proposed DSIM is shown in Fig. 7. The spectral efficiency is set to 0.8889 bits/s/Hz, which can be obtained by $N = 4$ and 8-PSK for DSIM scheme, and $M = 2$ for DPSK-OFDM scheme.

This article has been accepted for publication in a future issue of this journal, but has not been fully edited. Content may change prior to final publication. Citation information: DOI 10.1109/TVT.2018.2837691, IEEE Transactions on Vehicular Technology

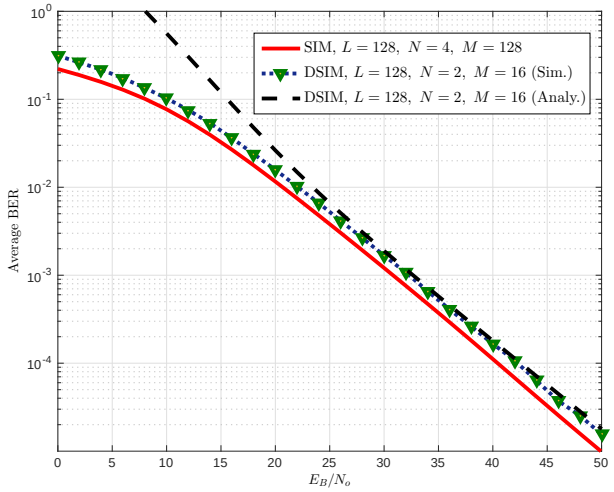

Fig. 6. The average BER versus E_b/N_o for IM-OFDM and DIM-OFDM at a spectral efficiency of 2 bps/Hz. ($L = 128$, $\nu = 10$, $C = 16$).

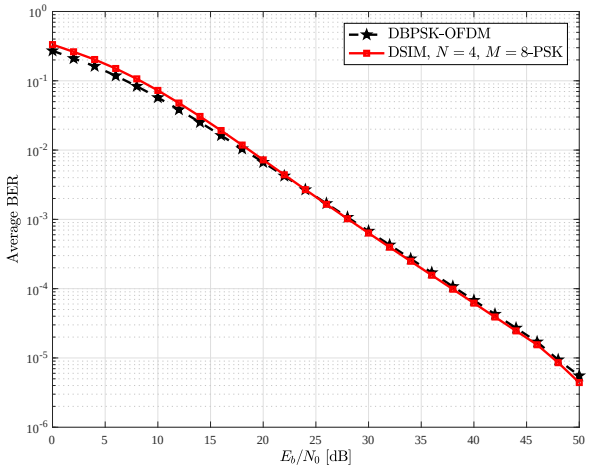

Fig. 7. The average BER versus the average SNR order for DBPSK-OFDM and DSIM ($N = 4$ and 8-PSK). ($L = 128$, $\nu = 10$, $C = 16$).

As clearly evident from the figure, both schemes demonstrate almost identical performance. A closer look highlights that DBPSK-OFDM system demonstrates a slight performance enhancement over DSIM at low SNR range, while DSIM achieves marginal gain at high SNR values. However, a detailed comparison among different non-coherent OFDM schemes is required to exploit the advantages of each scheme over the others. For instance, the complexity of DPSK-OFDM system is much lower than the proposed DSIM scheme. It is important to note that the proposed DSIM scheme cannot compete with DPSK-OFDM when increasing the modulation orders. Also, increasing M for DSIM will induce a high complexity due to the unitary constraint. However, SIM is shown to have many advantages over conventional OFDM schemes and witnessed tremendous research interest in the past few years. One major advantage is that SIM activates only a single subcarrier within each subgroup, whereas typical OFDM system activates all subcarriers. To this end, under specific scenarios, it has been proved in [42] that the PAPR will be reduced for SIM as compared to conventional OFDM system. However, the considered scenario in [42] has been assumed unrealistic in [43]. Nevertheless, SIM still has a major advantage against conventional OFDM represented by the robustness against the inter-carrier interference.

VI. Conclusions

A novel OFDM-based differential IM scheme has been presented in this paper. The achievable spectral efficiency and the bit error rate of the proposed scheme have been investigated and analyzed. An upper bound of the achievable bit error rate has been derived as a closed form expression. Compared to the coherent scheme, the performance loss, in terms of the required SNR to reach a target BER, of the proposed scheme is about 4 dB SNR. Simulation results have been also shown to validate the analytical results.

Future works may investigate the complexity reduction at the detection stage as proposed in [44] since ML detection includes a high complexity load especially for large values of N. Also, the permutation of the active subcarriers over time can be addressed, where it can be optimized for improving the error performance at the receiver.

References

[1] E. Basar, "Index modulation techniques for 5G wireless networks," *IEEE Commun. Mag.,* vol. 54, no. 7, pp. 168-175, July 2016

[2] E. Basar, M. Wen, R. Mesleh, M. Di Renzo, Y. Xiao and H. Haas, "Index modulation techniques for next-generation wireless networks," *IEEE Access,* vol. 5, no.1 , pp. 16693-16746, Sep. 2017.

[3] M. Wen, X. Cheng, and L. Yang, "Index Modulation for 5G Wireless Communications", Springer International Publishing, 2017.

[4] X. Cheng, M. Zhang, M. Wen, L. Yang, "Index modulation for 5G: striving to do more with less", *to appear*, available on arXiv:1712.06235 [cs.IT].

[5] RY. Mesleh, H. Haas, S. Sinanovic, C. W. Ahn, and S. Yun, "Spatial modulation", *IEEE Trans. Veh. Technol.,* vol. 57, no. 4, pp. 2228-2241, 2008.

[6] J. Jeganathan, A. Ghrayeb, L. Szczecinski, "Spatial modulation: Optimal detection and performance analysis", *IEEE Commun. Lett.*, vol. 12, no. 8, pp. 545-547, Aug. 2008

[7] S. Sugiura, S. Chen, L. Hanzo, "A unified MIMO architecture subsuming space shift keying OSTBC BLAST and LDC", *Proc. IEEE VTCFall,* pp. 1-5, Sep. 2010.

[8] J. Jeganathan, A. Ghrayeb, L. Szczecinski and A. Ceron, "Space shift keying modulation for MIMO channels," *IEEE Trans. Wireless Commun.,* vol. 8, no. 7, pp. 3692-3703, July 2009.

[9] R. Mesleh, S. S. Ikki and H. M. Aggoune, "Quadrature spatial modulation," *IEEE Trans. Veh. Technol.,* vol. 64, no. 6, pp. 2738-2742, June 2015.

[10] E. Basar, U. Aygolu, E. Panayirci, H. V. Poor, "Orthogonal frequency division multiplexing with index modulation", *IEEE Trans. Signal Process.,* vol. 61, no. 22, pp. 5536-5549, Nov. 2013.

[11] J. Zhang, Y. Wang, J. Zhang and L. Ding, "Polarization shift keying (PolarSK): system scheme and performance analysis", *IEEE Trans. Veh. Technol.* (under review), May 2017, Available [Online]: https://arxiv.org/abs/1705.02738

[12] S. Gao, M. Zhang and X. Cheng, "Precoded Index Modulation (PIM) for Multi-Input Multi-Output OFDM," in *IEEE Trans. Wireless Commun.*, vol. PP, no. 99, pp. 1-1. doi: 10.1109/TWC.2017.2760823

[13] R. Fan, Y. J. Yu and Y. L. Guan, "Generalization of orthogonal frequency division multiplexing with index modulation," *IEEE Trans. Wireless Commun.,* vol. 14, no. 10, pp. 5350-5359, Oct. 2015.

[14] M. Wen, X. Cheng, M. Ma, B. Jiao, and H. V. Poor, "On the achievable rate of OFDM with index modulation, *IEEE Trans. Signal Process.,* vol. 64, no. 8, pp. 1919-1932, Apr. 2016.

[15] L. Xiao, B. Xu, H. Bai, Y. Xiao, X. Lei, and S. Li, "Performance evaluation in PAPR and ICI for ISIM-OFDM systems, in proc. *2014 Int. Workshop on High Mobility Wireless Commun.,* Beijing, China, Nov. 2014, pp. 84-88.

[16] J. Zheng and H. Lv, "Peak-to-average power ratio reduction in OFDM index modulation through convex programming, *IEEE Commun. Lett.,* vol. 21, no. 7, pp. 1505-1508, July 2017.

[17] Y. Ko, "A tight upper bound on bit error rate of joint OFDM and multi-carrier index keying, *IEEE Commun. Lett.,* vol. 18, no. 10, pp. 1763-1766, Oct. 2014.

[18] J. Crawford and Y. Ko, "Low complexity greedy detection method with generalized multicarrier index keying OFDM, in proc. *2015 IEEE 26th Annu. Int. Symp. on Pers., Indoor, and Mobile Radio Commun. (PIMRC)*, Hong Kong, China, Aug. 2015, pp. 688-693.

[19] J. Crawford, E. Chatziantoniou, and Y. Ko, "On the SEP analysis of OFDM index modulation with hybrid low complexity greedy detection and diversity reception, *IEEE Trans. Veh. Technol.,* vol. 66, no. 9, pp. 8103-8118, Sep. 2017.

[20] A. I. Siddiq, "Low complexity OFDM-IM detector by encoding all possible subcarrier activation patterns, *IEEE Commun. Lett.,* vol. 20, no. 3, pp. 446-449, Mar. 2016.

[21] W. Li, H. Zhao, C. Zhang, L. Zhao, and R. Wang, "Generalized selecting sub-carrier modulation scheme in OFDM system, in *2014 IEEE Int. Conf. on Commun. Workshops,* June 2014, pp. 907-911.

[22] M. Wen, X. Cheng, and L. Yang, "Optimizing the energy efficiency of OFDM with index modulation, in proc. *IEEE Int. Conf. Commun. Syst., Macau,* China, Nov. 2014, pp. 31-35.

[23] M. Wen, E. Basar, Q. Li, B. Zheng, M. Zhang, "Multiple-mode orthogonal frequency division multiplexing with index modulation, *IEEE Trans. Commun.,* vol. 65, no. 9, pp. 3892-3906, Sep. 2017.

[24] M. Wen, B. Ye, E. Basar, Q. Li, F. Ji, "Enhanced orthogonal frequency division multiplexing with index modulation, *IEEE Trans. Wireless Commun.,* vol. 16, no. 7, pp. 4786-4801, July 2017.

[25] B. Zheng, M. Wen, E. Basar, F. Chen, "Multiple-input multiple-output OFDM with index modulation: Low-complexity detector design, *IEEE Trans. Signal Process.,* vol. 65, no. 11, pp. 2758-2772, June 2017.

[26] E. Basar, "On multiple-input multiple-output OFDM with index modulation for next generation wireless networks, *IEEE Trans. Signal Process.,* vol. 64, no. 15, pp. 3868-3878, Aug. 2016.

[27] Y. Bian, X. Cheng, M. Wen, L. Yang, H. V. Poor and B. Jiao, "Differential spatial modulation," *IEEE Trans. Veh. Technol.,* vol. 64, no. 7, pp. 3262-3268, July 2015.

[28] M. Zhang, M. Wen, X. Cheng and L. Yang, "A Dual-Hop Virtual MIMO Architecture Based on Hybrid Differential Spatial Modulation," in *IEEE Trans. Wireless Commun.*, vol. 15, no. 9, pp. 6356-6370, Sept. 2016.

[29] N. Ishikawa and S. Sugiura, "Rectangular differential spatial modulation for open-loop noncoherent massive-MIMO downlink," *IEEE Trans. Wireless Commun.,* vol. 16, no. 3, pp. 1908-1920, March 2017

[30] J. Liu, L. Dan, P. Yang, L. Xiao, F. Yu and Y. Xiao, "High-rate APSK-aided differential spatial modulation: design method and performance analysis," *IEEE Commun. Lett.,* vol. 21, no. 1, pp. 168-171, Jan. 2017.

[31] P. A. Martin, "Differential spatial modulation for APSK in time-varying fading channels," *IEEE Commun. Lett.,* vol. 19, no. 7, pp. 1261-1264, July 2015.

[32] R. Mesleh; S. Althunibat; A. Younis, "Differential quadrature spatial modulation," *IEEE Trans. Commun.,* vol. 65, no. 9, pp. 3810-3817, Sept. 2017.

[33] K. S. Woo, K. I. Lee, J. H. Paik, K. W. Park, W. Y. Yang and Y. S. Cho, "A DSFBC-OFDM for a next generation broadcasting system with multiple antennas," *IEEE Trans. on Broadcast.*, vol. 53, no. 2, pp. 539-546, June 2007.

[34] B. L. Hughes, "Differential space-time modulation," *IEEE Trans. Inform. Theory,* vol. 46, no. 7, pp. 2567-2578, Nov 2000.

[35] P. A. Martin, "Differential spatial modulation for APSK in time-varying fading channels," *IEEE Commun. Lett.*, vol. 19, no. 7, pp. 1261-1264, July 2015.

[36] S. Sugiura, C. Xu, S. X. Ng, L. Hanzo, "Reduced-complexity coherent versus non-coherent QAM-aided space-time shift keying", *IEEE Trans. Commun.,* vol. 59, no. 11, pp. 3090-3101, Nov. 2011.

[37] http://en.wikipedia.org/wiki/Stirlings approximation

[38] M.K. Simon et al., "*Digital Communication Techniques: Signal Design and Detection*", Prentice Hall PTR, 1995.

[39] J. G. Proakis, *Digital Communications*. McGrawHill, 1995.

[40] J. Craig, "A new, simple, and exact result for calculating the probability of error for two-dimensional signal constellations, in *Proc. IEEE MILCOM,* 1991, pp. 571-575.

[41] G. L. Turin, "The characteristic function of hermitian quadratic forms in complex normal variables, *Biometrika,* vol. 47, no. 1/2, pp. 199-201, Jun 1960.

[42] D. Tsonev, S. Sinanovic, and H. Haas, "Enhanced subcarrier index modulation (SIM) OFDM,, *IEEE GLOBECOM Workshops,* Houston, TX, USA, Dec. 2011, pp. 728732.

[43] H. Ochiai and H. Imai, "On the distribution of the peak-to-average power ratio in OFDM signals, *IEEE Trans. Commun.,* vol. 49, no. 2, pp. 282-289, 2001.

[44] L. Xiao et al., "A low-complexity detection scheme for differential spatial modulation," *IEEE Commun. Lett.*, vol. 19, no. 9, pp. 1516-1519, Sept. 2015.

Saud Althunibat received his Ph.D. degree in Telecommunications from the University of Trento (Italy) in 2014. Currently, he is an assistant professor at Al-Hussein Bin Talal University (Jordan), and serves as the head of the Communications Engineering Department. He serves as a General Co-Chair of BROADNETs 2018 conference. He has authored more than 50 scientific papers. He has received the best paper award in IEEE CAMAD 2012, and was selected as Exemplary Reviewer for IEEE Communications Letters in 2013. His research interests include a wide range of wireless communication topics such as, index modulation, spectrum sharing, cognitive radio, wireless sensor networks, energy efficiency and resource allocation.

Raed Mesleh joined German Jordanian university in Amman, Jordan, in February 2015 where he is currently the vice dean of the school of electrical engineering and information technology and an associate professor at the department of Electrical and Communication Engineering. He received his PhD in 2007 from Jacobs University in Bremen, Germany. From 2007 to 2010 he was a postdoctoral fellow at Jacobs University. He was with the Electrical Engineering Department at University of Tabuk in Saudi Arabia from 20102015. He was a visiting scholar at Boston University, The University of Edinburgh and HerriotWatt University. In December 2016, he was awarded the Arab Scientific Creativity award from Arab Thought Foundation.

Ertugrul Basar (S'09-M'13-SM'16) received the B.S. degree (Hons.) from Istanbul University, Turkey, in 2007, and the M.S. and Ph.D. degrees from Istanbul Technical University in 2009 and 2013, respectively. From 2011 to 2012, he was with the Department of Electrical Engineering, Princeton University, Princeton, NJ, USA as a visiting research collaborator. He was an Assistant Professor with Istanbul Technical University from 2014 to 2017, where he is currently an Associate Professor of Electronics and Communication Engineering. His primary research interests include MIMO systems, index modulation, cooperative communications, OFDM, and visible light communications. Dr. Basar currently serves as an Associate Editor of IEEE COMMUNICATIONS LETTERS and IEEE ACCESS, and as an Editor of *Physical Communication (Elsevier).*